Supplementary Material S1 to "Effects of lake-reservoir pumped-storage operations on temperature and water quality"

Ulrike Gabriele Kobler [1,*], Alfred Wüest [1,2] and Martin Schmid [1]

[1] Eawag, Swiss Federal Institute of Aquatic Science and Technology, Surface Waters – Research and Management, CH-6047 Kastanienbaum, Switzerland; ulrike.kobler@eawag.ch, alfred.wueest@eawag.ch, martin.schmid@eawag.ch

[2] EPFL. Physics of Aquatic Systems Laboratory – Margaretha Kamprad Chair, ENAC-IEE-APHYS, CH-1015 Lausanne, Switzerland; alfred.wueest@epfl.ch

* Correspondence: ulrike.kobler@eawag.ch; Tel.: +41 58 765 2210

Sustainability 2018, 10, 1968; doi:10.3390/su10061968 www.mdpi.com/journal/sustainability

A. Model forcing and initial conditions

A.1. Bathymetry

The bathymetry is based on Lidar measurements (terra Vermessungen, October 2014, personal communication) for Sihlsee and on GIS-data of the Federal Institute of Topography (swisstopo Art. 30 GeoIV: 5704 000 000 / DHM25@2003) for Upper Lake Zurich.

Both water basins are divided into 200 m wide segments along the main axis and 0.5-m thick layers (depth). This results in 43 (58) segments and 47 (93) layers for Sihlsee (Upper Lake Zurich). The numbers of segments and layers include at each margin a segment or layer filled with zeros. An overview of the model grid with the positions of all in-, out- and artificial flows is given in Figure A1.

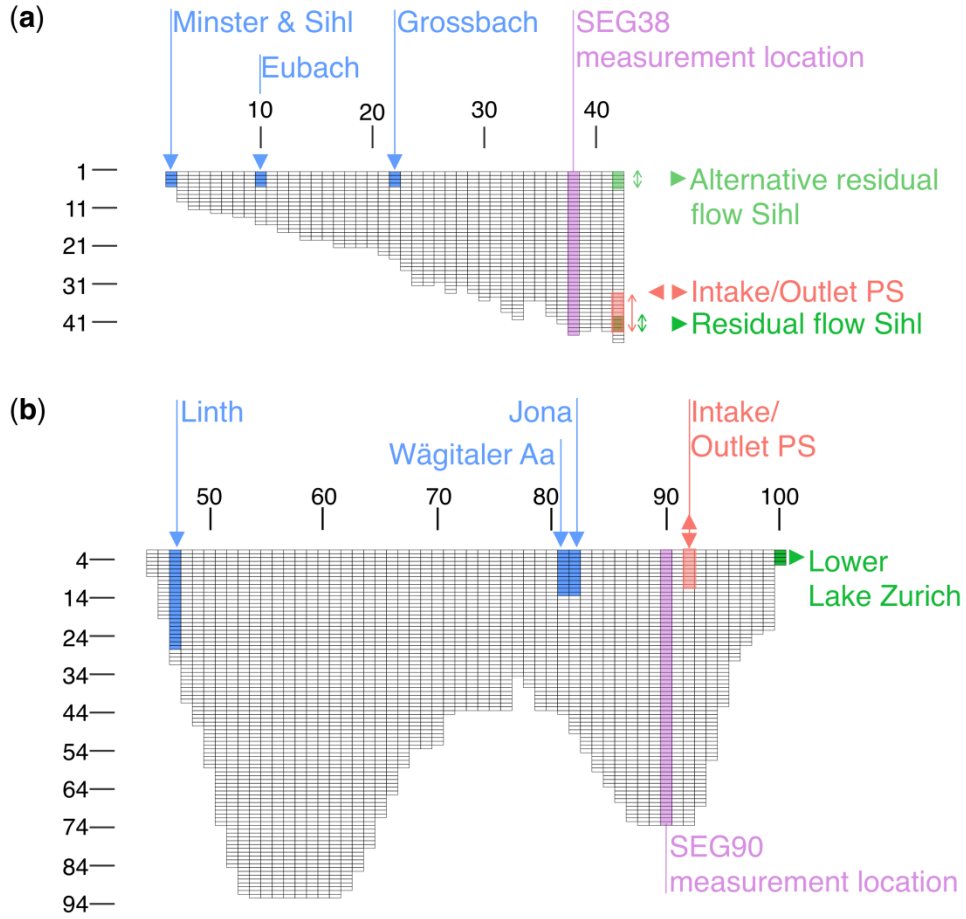

Figure A1. Overview of model grid: Sihlsee (a) and Upper Lake Zurich (b) including the positions of all inflows (blue), outflows (green) and artificial flows (red). The grid labels indicate segment numbers on the horizontal and layer numbers on the vertical axis. The segments with available observations (SEG38 and SEG90) are shaded in violet.

The Sihlsee inflows are located in segments 2 (Minster and Sihl), 10 (Eubach) and 22 (Grossbach), each entering the lake within the top 4 layers. At Upper Lake Zurich the inflows are located in segments 4 (Linth), 37 (Wägitaler Aa) and 38 (Jona). While River Linth is distributed into layers 2-28, the other inflows enter between layers 2-14. The outflow to Lower Lake Zurich is located at segment 58 and implemented as a weir.

The PS intake and outlet of present and extended PS at Sihlsee is located at segment 42 and stretches from layer 33 to 43, that at Upper Lake Zurich is positioned at segment 49 and extends between layers 2 to 12.

The residual flow to River Sihl from Sihlsee is indicated in green in Figure A1. The regular outlet is located at segment 42 between layers 38 to 43, where water is withdrawn for the present PS, the extended PS scenario and the reference scenario NoPS. For the reference scenario QNat the outlet of the residual flow is moved to the surface (weir crest at 887.4 m a.s.l.).

A.2. Meteorological Forcing

For calculating heat exchange at the water surface and mixing processes, the standard version of CE-QUAL-W2 requires the input of air temperature, dew point, wind speed and direction as well as cloudiness and solar radiation. Incoming long-wave radiation is then calculated internally. We replaced this procedure with an external calculation of long-wave radiation and modified the code to read in these values instead of cloudiness, which is then no longer required. Long-wave radiation was calculated according to recommendations given by Flerchinger, *et al.* [1]. Incoming clear-sky long-wave radiation was calculated using the method of Dilley and O'Brien [2]. The cloud correction by Unsworth and Monteith [3], and the elevation correction by Deacon [4] were applied. The albedo of long-wave radiation was kept constant at 0.97.

Table A1. Overview of meteorological information used. Shown are the temporal resolution (h: hourly, d: daily), the time range which was used to generate the meteorological forcing and the order of stations of MeteoSwiss, which were used to fill data gaps: (1) Zurich Fluntern, (2) Wädenswil, (3) Schmerikon and (4) Einsiedeln.

Water body	Variable	Temporal resolution	Time period	Station	Institution	Gap treatment
Upper Lake Zurich	Air temperature	h	01.01.1997-31.12.2015	Wädenswil	MeteoSwiss	(1)
	Dew point	h	01.01.1997-31.12.2015	Wädenswil	MeteoSwiss	(1)
	Wind velocity	h	01.01.1997-31.12.2015	Schmerikon	MeteoSwiss	(2), (1)
	Wind direction	h	01.01.1997-31.12.2015	Schmerikon	MeteoSwiss	(2), (1)
	Cloudiness	d	01.01.1997-31.12.2015	Wädenswil	MeteoSwiss	(1)
	Solar radiation	h	01.01.1997-31.12.2015	Wädenswil	MeteoSwiss	(1)
Sihlsee	Air temperature	h	01.01.1997-31.01.2007	Einsiedeln	MeteoSwiss	(2), (1)
		h	01.02.2007-31.12.2015	Einsiedeln	Segelclub Sihlsee	(4), (2), (1)
	Dew point	h	01.01.1997-31.01.2007	Einsiedeln	MeteoSwiss	(2), (1)
		h	01.02.2007-31.12.2015	Einsiedeln	Segelclub Sihlsee	(4), (2), (1)
	Wind velocity	h	01.01.1997-31.01.2007	Wädenswil	MeteoSwiss	(1)
		h	01.02.2007-31.12.2015	Einsiedeln	Segelclub Sihlsee	(4), (2), (1)
	Wind direction	h	01.01.1997-31.01.2007	Wädenswil	MeteoSwiss	(2), (1)
		h	01.02.2007-31.12.2015	Einsiedeln	Segelclub Sihlsee	(4), (2), (1)
	Cloudiness	d	01.01.1997-29.04.2012	Einsiedeln	MeteoSwiss	(1)
		d	30.04.2012-31.12.2015	Wädenswil	MeteoSwiss	(1)
	Solar radiation	h	01.01.1997-07.03.2012	Wädenswil	MeteoSwiss	(1)
		h	08.03.2012-31.12.2015	Einsiedeln	MeteoSwiss	(2), (1)

The meteorological forcing for Sihlsee was mostly based on observations of MeteoSwiss at Einsiedeln and Segelclub Sihlsee (Figure 1, Table A1). Monitoring of solar radiation and wind speed at an hourly time step at Einsiedeln started only in 2007. For previous years data from the MeteoSwiss station Wädenswil were used. In 2012 the measurement of cloudiness at Einsiedeln was discontinued. Afterwards data were taken from the MeteoSwiss station Zurich Fluntern.

For Upper Lake Zurich, observations of the MeteoSwiss station Wädenswil were used for air temperature, dew point, cloudiness and solar radiation. Wind velocity and direction were taken from the MeteoSwiss station Schmerikon (Figure 1, Table A1). Gaps were filled with data from the closest station (Wädenswil, followed by Zurich Fluntern).

A.3. Hydrological Forcing

For Sihlsee, the discharges of the rivers Minster, Eubach and Grossbach are monitored by the Federal Office for the Environment (FOEN). As inflows of River Sihl and the remaining catchment area were not available, these were estimated by scaling the inflow of Minster proportional to their catchment area. The outflows to River Sihl for present and extended PS are based on simulations of the Swiss Federal Institute for Forest, Snow and Landscape Research [5]. These simulations give the total flow in River Sihl downstream of the dam, composed of the sum of discharges through the regular outlet and those of floods over the spillway. Since all water is withdrawn from the bottom outlet in the model, the simulated flow patterns during flood events may be different to those actually occurring in the reservoir.

The outflow of the two reference scenarios (QNat and NoPS) is based on a modelling study of LIMNEX AG (personal communication). In case of QNat the outflow is implemented using a weir (Figure A1, upper edge at 884.7 m a.s.l., 5 m wide, weir discharge coefficient 0.7) which directly allows the computation of the discharge following the formula of Poleni [6]. For NoPS, the discharge computed with CE-QUAL-W2 for QNat was used, but withdrawn from the hypolimnion instead of being discharged over a weir (Figure A1). Figure A2 depicts the PS flows as well as the residual flow to river Sihl for the reference scenarios QNat and NoPS, the present PS and the extended PS scenarios.

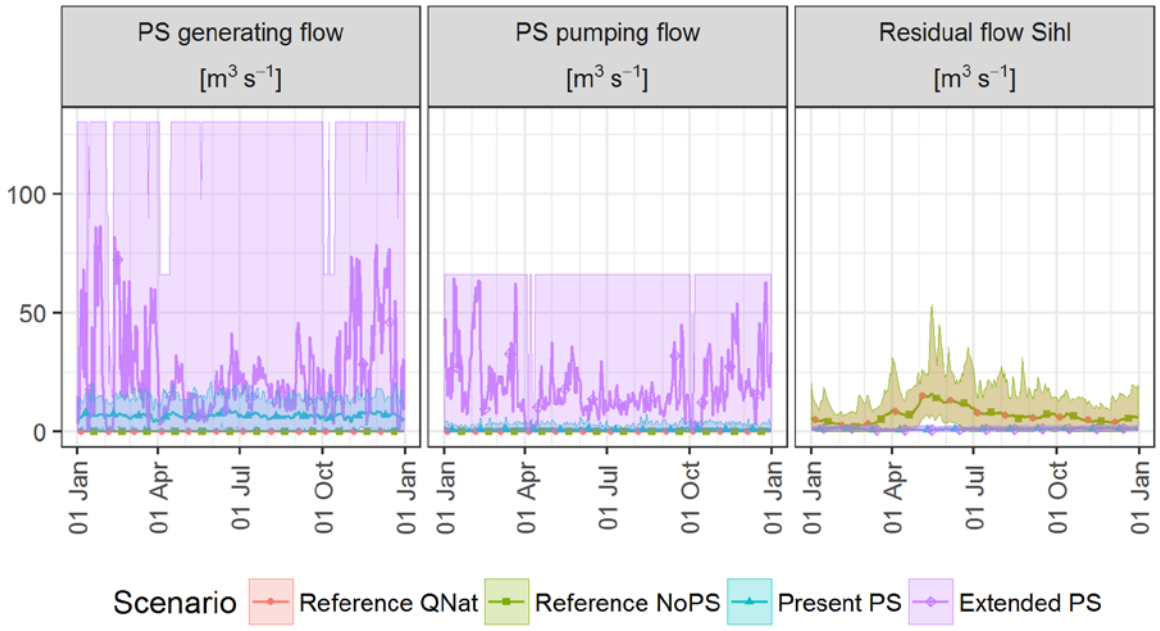

Figure A2. PS generating and PS pumping flow as well as residual flow to river Sihl ($m^3 s^{-1}$) for the reference scenario QNat and NoPS, the present PS and the extended PS scenario. Shown are means (lines with markers) and range of minima and maxima (shaded areas) of simulated years 1998-2012.

To account for measurement errors as well as missing inflows, groundwater exchange, evaporation and precipitation at Sihlsee we estimated a correction term to achieve agreement with observed water levels. Simulated and observed water levels were converted to the corresponding volume for each day, and their difference was averaged for each month. The monthly missing volume was then implemented as a distributed tributary, which could also have negative values.

Of the inflows to Upper Lake Zurich, only the discharge of River Linth at Weesen is routinely monitored by FOEN. As no additional information was available, this discharge was used to scale the other inflows by the corresponding ratio of catchment area. The outflow to Lower Lake Zurich was implemented through a weir (upper edge at 405.5 m a.s.l., 200 m wide, weir discharge coefficient 0.5).

Both scenario-independent and scenario-dependent hydrological forcing of Sihlsee and Upper Lake Zurich are given in Table 1. While no PS flows are withdrawn in case of the reference scenarios (NoPS and QNat), extended PS increases PS generating and PS pumping flows by factors of ~4 and ~22, respectively (Figure A2). Based on the hydrological forcing the average water residence time in Sihlsee can be estimated to 150 days for the reference scenarios, 135 days for present PS and 40 days for extended PS.

The basic dataset of hourly exchange flows for the extended PS scenario was provided by the Swiss Federal Railways and considered monthly-averaged net inflows to Sihlsee. It needed adaptation to allow assessing the influence of floods and low flows. Thus, the PS flows of the extended PS scenario were adapted based on the formulation of an hourly water balance, with hourly natural in- and outflows, where the resulting water level is limited by minimum and maximum operational water levels as well as temporal restrictions for the minimal water level from June to October.

A.4. Inflow Water Quality Forcing

FOEN provides water temperature observations at Rivers Alp and Linth for the considered simulation period (Figure 1). The River Alp was chosen to be representative for all inflows of Sihlsee and the River Linth for those of Upper Lake Zurich. Inflow temperatures for Sihlsee range from ~1 °C in winter to ~18 °C in summer. River Linth is the outflow of Walensee and thus significantly warmer in winter with average temperatures ~6 °C.

Inorganic suspended solid concentrations of the inflows of Sihlsee were estimated based on Keller and Weibel [7]. They derived an empirical relationship between stream flow in mm per week and suspended solid concentrations in mg-L^{-1} for two sub-catchments of River Alp. Out of the two, Erlenbach (referred to as 10 in their publication) was chosen as it corresponds better to the catchment of Sihlsee. Thus, the regression listed on page 57 of their publication was used to estimate inorganic suspended solid concentrations for all inflows of Sihlsee. Inorganic suspended solid concentrations of the inflows of Upper Lake Zurich were estimated as follows: for Linth, Peters-Kümmerly [8] determined a direct relationship between discharge and the load of suspended solids. The estimated regression follows Eq.1.

$$c = 1.15 \cdot Q^{0.04}, \quad (1)$$

with c in mg L^{-1} and Q in m^3 s^{-1}. Additional information for the other inflows to Upper Lake Zurich was missing, thus inorganic suspended solid concentrations were estimated with the same procedure as for Sihlsee. When calibrating the model, inorganic suspended solid concentrations were scaled for both water bodies with the parameter f_{ISS}.

Dissolved oxygen concentrations were estimated according to Haynes [9], assuming equilibrium with the atmosphere, using the water temperature of the inflows. Nutrient concentrations of the sum of nitrate and nitrite, ammonium and phosphate were considered as forcing for all the inflows. For Sihlsee, these were approximated with observations at Erlenbach, a sub-catchment of River Alp (Figure 1). There nitrate, total nitrogen and phosphate have been observed weekly as part of a national monitoring program (NADUF) since 2003. Ammonium, not directly observed, was approximated by the difference of total nitrogen and nitrate. Weekly

averages of all years between 2003-2015 were used to generate a mean annual forcing, which was assigned to the nutrient forcing for all simulated years. During model calibration these time series were scaled with the parameters f_{PO4}, f_{NO} and f_{NH4} (Section B.2). For Upper Lake Zurich, the mean annual nutrient concentrations were calculated based on monthly observations in River Linth (1997-2014). As the observations of the other inflows to Upper Lake Zurich are not as comprehensive, these average annual nutrient concentrations were also assigned to the nutrient forcing of the other inflows. The parameters f_{PO4}, f_{NO} and f_{NH4} (Section B.2) were adjusted during model calibration to scale the water quality time series for Linth and the other two inflows separately, as the concentrations differ substantially according to Gammeter and Forster [10].

A.5. Initial conditions

The initial conditions for both water bodies are given in Table A2. The model was initialized on 01 January. At this time, Upper Lake Zurich is usually homogenized, while Sihlsee is inversely stratified. For Upper Lake Zurich, constant values corresponding to average observed winter conditions or to default values of CE-QUAL-W2 were set as initial conditions. For Sihlsee, an inversely stratified temperature profile was assumed, whereas water quality parameters were set to constant values. The first year of the simulations was excluded from the analysis, and due to the relatively short residence times, the initial conditions have only a minor impact on the simulation results in the subsequent years.

Table A2. Initial conditions of temperature, ice thickness and concentrations of inorganic suspended solids, phosphate, ammonium, sum of nitrate and nitrite, labile dissolved organic matter (LDOM), refractory dissolved organic matter (RDOM), labile particulate organic matter (LPOM), refractory particulate organic matter (RPOM), algal groups 1 and 2, dissolved oxygen and zooplankton. Temperature at Sihlsee was input as profile.

		Sihlsee										Upper Lake Zurich
Variable	**Layer**	**2-46**	**2**	**3**	**4**	**5**	**6**	**7**	**8**	**9**	**10-46**	**2-92**
	Unit											
Temperature	[°C]		0.8	0.9	1	1.5	2	2.5	3	3.5	4	6
Ice thickness	[m]	0.1										0
Inorg. suspended solids	[mg L^{-1}]	2										2
Phosphate	[µg P L^{-1}]	5										5
Ammonium	[µg N L^{-1}]	2										2
Sum of nitrate and nitrite	[µg N L^{-1}]	300										700
LDOM	[mg L^{-1}]	0.1										0.1
RDOM	[mg L^{-1}]	0.1										0.1
LPOM	[mg L^{-1}]	0.1										0.1
RPOM	[mg L^{-1}]	0.1										0.1
Algae group 1	[mg L^{-1}]	0.05										0.05
Algae group 2	[mg L^{-1}]	0.05										0.05
Dissolved oxygen	[mg L^{-1}]	10										11
Zooplankton	[mg L^{-1}]	0.01										0.01

B. Available observations at Sihlsee and Upper Lake Zurich and model calibration

B.1. Available observations

The observations at Sihlsee, were conducted by Eawag solely for the purpose of this study from April 2014 to December 2016. Temperatures, observed quasi-continuously (Figure B1), show that seasonal convective mixing occurred latest in mid-October, and inverse stratification started to evolve at end-December, facilitating ice growth dependent on meteorological conditions. In winter 2014/15 the lake was ice covered, but not in winter 2015/16. Summer stratification arose between beginning and mid-April with maximum temperatures between 20 and 25 °C and 15 to 17 °C in the epi- and hypolimnion, respectively. Summer hypolimnion temperatures are high compared to most stratified Swiss lakes, where they generally remain below 10 °C throughout the year. As shown in the present study, these high hypolimnion temperatures are caused by deep water withdrawal in the lake.

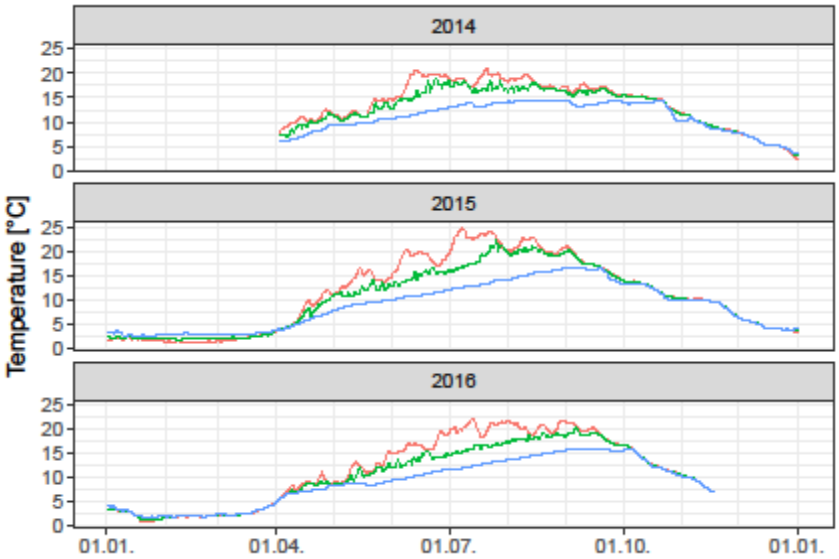

Figure B3. Observed water temperature in Sihlsee for 2014-2016 at three depths: 1 m below surface (red), 6 m below surface (green), 0.5 m above sediment (blue); measurements were performed at SEG38 (Figure 1).

Vertical profiles of additional physical and chemical parameters were measured on a monthly basis from April 2014 to December 2016 (26 profiles for inorganic suspended solids and nitrate, 25 for dissolved oxygen, 16 for Chlorophyll-a, 24 for total phosphorus). Observed inorganic suspended solid concentrations were homogeneously distributed at ~5 mg L^{-1} in April and from October to December. During summer stratification inorganic suspended solid concentrations were ~5 and <30 mg L^{-1} in the epi- and the hypolimnion, respectively. One flood event on 22 July 2014 caused ISS concentration peaks in the thermocline. In August and September, dissolved oxygen concentrations in the hypolimnion fell below 4 mg L^{-1}, the legal requirement in Switzerland [11]. Chlorophyll-a concentrations did not exceed 3.5 µg L^{-1}, with highest values for June, August and September. Observed nitrate concentrations varied between 100 and 350 µg N L^{-1}, with decreased concentrations in the epilimnion due to algal uptake from June to September. Nitrite concentrations were <10 µg N L^{-1} for the 2 observations made. Total phosphorus was <35 µg P L^{-1}, with enriched concentrations in the hypolimnion for July and September and epilimnion concentrations <10 µg P L^{-1} throughout the year. Thus, Sihlsee can be considered oligotrophic.

The observations at Upper Lake Zurich are part of a monitoring program by the cantonal agencies [10,12]. The observed temperature (1994-2005) during summer stratification was 5-6 °C and 20-25 °C for the hypo- and the epilimnion, respectively [10]. From December to April, the lake was mixed and in some winters inversely stratified with a minimum surface temperature of ~2 °C. Wind protected bays can freeze over during very cold winters [10]. No observations are available for inorganic suspended solid concentrations. The hypolimnetic dissolved oxygen concentrations at SEG90 (Figure 1) for 1994-2005 fell below 4 mg L^{-1} every year during the stagnation period. Chlorophyll-a concentrations did not exceed 6 µg L^{-1} for 2006-2010. The mean annual concentrations (1996-2010) of nitrate, nitrite and ammonium were 700, 5 and 10 µg N L^{-1} and those of orthophosphate were ~10 µg P L^{-1}. The annual mean of the total phosphorus concentrations did not exceed 12 µg P L^{-1}. Thus, Upper Lake Zurich can be classified as mesotrophic.

B.2. Model Calibration

The model was calibrated manually with a manual trial and error approach, with the aim of minimizing root mean square errors (RMSE), mean absolute errors (MAE) and mean errors (ME) between simulated and observed quantities. Additionally, the differences between observed profile and time series data and simulations were visually inspected. Several model parameters of

CE-QUAL-W2 and factors for adjusting the water quality forcing (Section A) of both water bodies were calibrated, while the majority of the other parameters was either set to the default value or determined based on literature values [13-15].

RMSEs are given in Table 2 of the main manuscript, MAEs and MEs in Table B1. Moreover, temperature profiles at Sihlsee and Upper Lake Zurich show a good agreement for the calibration period (2014-2015) (Figure B2, Figure B3). Similar to the RMSEs (Table 2) MAEs and MEs shows that dissolved oxygen and nutrient concentrations are better predicted in the epi- than in the hypolimnion.

The comparison of simulated and observed ice-thickness is show in Figure B4, where observations were provided by the Swiss Federal Railways, and volumetrically averaged time series of observed and simulated variables for epi- and hypolimnion are shown in Figure B5 and B6 for Sihlsee and Upper Lake Zurich, respectively. While in the epilimnion concentrations are either overestimated (sum of nitrate and nitrite) or underestimated (total phosphorus), the average in the hypolimnion is reproduced satisfactorily. The model is, however, not capable of reproduction peak concentrations, which typically occur during floods. A list of model parameters with a description, and their corresponding default and calibrated values are given in Table B2.

Table B3. Mean absolute error (MAE) and mean error (ME) of temperature, dissolved oxygen, the sum of nitrate and nitrite as well as total phosphorus computed for the entire water column, the epilimnion and the hypolimnion of Sihlsee or Upper Lake Zurich (na: not available).

Variable	Unit	Sihlsee 2014-2015			Upper Lake Zurich 1998-2015		
		Entire water column	Epi-limnion [1]	Hypo-limnion [2]	Entire water column	Epi-limnion [1]	Hypo-limnion [3]
Mean absolute error (MAE)							
Temperature	[°C]	0.71	0.69	0.75	0.63	0.54	0.65
Dissolved oxygen	[mg L^{-1}]	0.90	0.82	1.05	0.98	0.83	0.93
Inorg. suspended solids	[mg L^{-1}]	2.78	1.13	4.34	na	na	na
Sum of nitrate and nitrite	[µg N L^{-1}]	61	58	69	91	114	91
Total phosphorus	[µg P L^{-1}]	2.86	2.03	4.14	2.95	2.96	2.88
Mean error (ME)							
Temperature	[°C]	0.41	0.58	0.28	-0.11	0.02	-0.23
Dissolved oxygen	[mg L^{-1}]	0.36	-0.10	0.94	0.49	0.00	0.35
Inorg. suspended solids	[mg L^{-1}]	1.55	0.56	1.90	na	na	na
Sum of nitrate and nitrite	[µg N L^{-1}]	21	14	18	16	70	26
Total phosphorus	[µg P L^{-1}]	-1.20	-0.76	-2.64	-1.75	-2.03	-1.76

[1] Uppermost 5 m of the water column. [2] Lowermost 5 m of the water column. [3] All depths ≥ 20 m.

Table B2. Model parameters deviating from the default values of CE-QUAL-W2. Given are the values for both water bodies and the default value of CE-QUAL-W2. The column on the right indicates whether the parameters where selected from literature (in capital letters) or computed by calibration (cal). The capital letters stand for: A: Bonalumi, *et al.* [14], B: Mieleitner and Reichert [13], C: Mieleitner and Reichert [15].

		Sihlsee	Upper Lake Zurich	Default	Based on
Inorganic suspended solids					
SSS	Settling velocity [m d^{-1}]	0.2	0.2	1	
SEDRC	Sediment resuspension	ON	ON	OFF	A
TAUCR	Critical shear stress for sediment resuspension	0.001	0.001	1	
Gas exchange					
EQN#	Equation used to calculate gas exchange	5	5	6	A
Parameters nitrification and denitrification					
NH4T1	Lower temperature for ammonia decay [°C]	0	0	5	cal
NO3T1	Lower temperature for nitrate decay [°C]	0	0	5	

Continuation Table B2.

		Sihlsee	Upper Lake Zurich	Default	Based on
Parameters nitrification and denitrification					
ORGP	Organic matter stoichiometric coefficient for phosphorus [-]	0.0087	0.0087	0.005	B
ORGN	Organic matter stoichiometric coefficient for nitrogen [-]	0.08	0.08	0.08	cal
Parameters organic matter					
OMT1	Lower temperature for organic matter decay [°C]	0	0	4	cal
OMT2	Upper temperature for organic matter decay [°C]	30	30	25	
Parameters sediment					
NH4R	Sediment release rate of ammonium, fraction of SOD-rate	0.02	0.02	0.001	cal
SEDC	Detailed sediment- diagenesis-model	ON	ON	OFF	
SEDCI	Initial sediment concentration [g m^{-2}]	0.01	0.01	0	
SOD	Anaerobic sediment release rate [g m^{-2} d^{-1}]	0.4	1		
DYNSEDK	Dynamic computation first-order-model	ON	ON	OFF	
SODT1	Lower temperature for sediment decay [°C]	0	0	4	
Mixing parameters					
FRIC	Chézy friction coefficient [$m^{0.5}$ s^{-1}]	70	70		A
AX	Longitudinal Eddy-Viscosity [m^2 s^{-1}]	0.1	0.1	1	
DX	Longitudinal Eddy-Diffusivity [m^2 s^{-1}]	0.1	0.1	1	
AZMAX	Maximum vertical Eddy-Viscosity [m^2 s^{-1}]	0.1	0.1	1	
FI	Internal friction [-]	0.01	0.01	0.015	
Scaling of meteorological forcing					
SHD	Shading coefficient [-]	0.85	0.90	1	cal
WSC	Wind sheltering coefficient [-]	1.35	1.25	1	
Scaling of water quality forcing of inflows					
f_{ISS}	Multiplier inorganic suspended solids [-]	0.25	1.00 | 0.25[1]		cal
f_{PO4}	Multiplier phosphate [-]	4.58	1.00 | 32.5[1]		
f_{NH4}	Multiplier ammonium [-]	0.17[2]	0.65 | 0.72[1]		
f_{NO}	Multiplier nitrate + nitrite [-]	1.42	1.10 | 4.86[1]		
Heat exchange at air water interface					
AFW	Coefficient wind function [W m^{-2} mm Hg^{-1}]	5.87	5.87	9.2	A
BFW	Coefficient wind function [W m^{-2} mm Hg^{-1} (m s^{-1})$^{-CFW}$]	2.42	2.42	0.46	
CFW	Coefficient wind function	1	1	2	
Heat exchange at sediment water interface					
TSED	Temperature sediment [°C]	5	7	10	cal
CBHE	Coefficient heat exchange [W m^{-2} $°C^{-1}$]	$1.0x10^{-6}$	$1.0x10^{-6}$	0.3	A
Light attenuation water column					
EXH2O	Attenuation pure water [m^{-1}]	0.2	0.2	0.25	cal
BETA	Fraction incident solar radiation absorbed at water surface [-]	0.35	0.35	0.45	

[1] The two multipliers for inflow water quality at Upper Lake Zurich were used for River Linth and the other two inflows (Jona and Wägitaler Aa), respectively.

[2] As ammonium was not observed, the difference of total nitrogen and nitrate and nitrite was taken as proxy and adapted with the given factor.

Continuation Table B2.

		Sihlsee / Upper Lake Zurich			Based on
		Group 1	**Group 2**	**Default**	
Parameters phytoplankton					
AG	Max. growth rate phytoplankton [d^{-1}]	1.9	1.4	2	cal/C
AR	Max. respiration rate phytoplankton [d^{-1}]	0.05	0.05	0.04	B
AE	Max. excretion rate phytoplankton [d^{-1}]	0.015	0.015	0.04	cal
AM	Max. mortality rate phytoplankton [d^{-1}]	0.015	0.015	0.1	cal
AS	Algal settling rate [m d^{-1}]	0.08	0.01	0.1	C
ALGP	Algal stoichiometric coefficient for phosphorus [-]	0.0087	0.0087	0.005	B
ALGN	Algal stoichiometric coefficient for nitrogen [-]	0.08	0.08	0.08	cal
ALPOM	Fraction of algal biomass converted to POM when dying	0.9	0.9	0.8	B
AHSP	Algal half-saturation for phosphor [g m^{-3}]	0.0007	0.0013	0.003	C
AT1	Lower temperature for algal growth [°C]	0	0	5	cal
AT2	Lower temperature for max. algal growth [°C]	11	11	25	
AT3	Upper temperature for max. algal growth [°C]	15	15	35	
AT4	Upper temperature for algal growth [°C]	30	30	40	
ACHLA	Ratio algal biomass to chlorophyll a [mg Algae (µg Chl a)$^{-1}$]	0.1	0.1	0.05	
Parameters zooplankton					
ZG	Max. growth rate zooplankton [d^{-1}]	0.7		1.5	cal
ZP	Zooplankton stoichiometric coefficient for phosphorus [-]	0.0087		0.005	B
ZN	Zooplankton stoichiometric coefficient for nitrogen [-]	0.08		0.08	cal
ZT1	Lower temperature for zooplankton growth [°C]	0		5	
ZT2	Lower temperature for max. zooplankton growth [°C]	20		25	
ZT3	Upper temperature for max. zooplankton growth [°C]	30		35	
ZT4	Upper temperature for zooplankton growth [°C]	35		40	

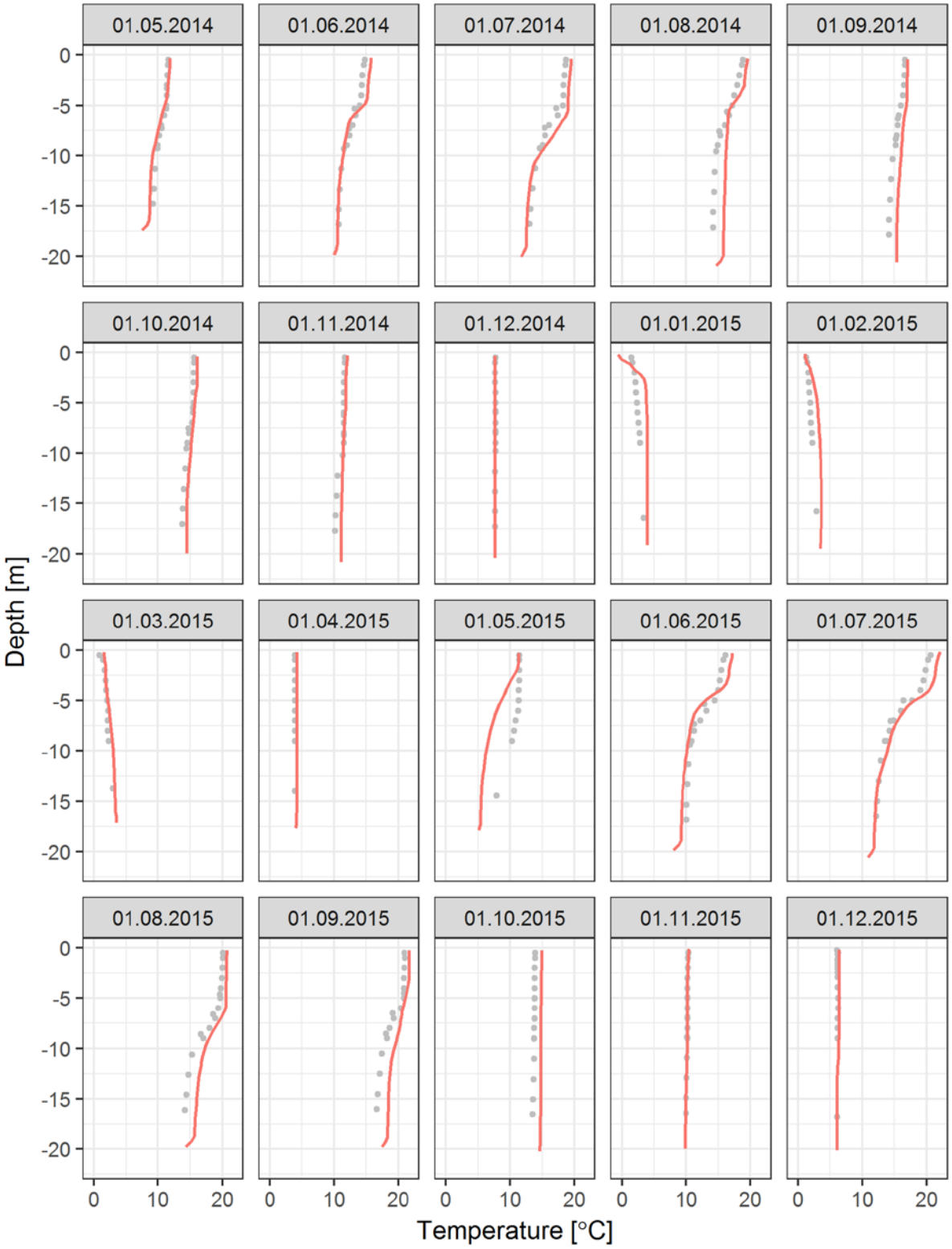

Figure B4. Simulated (red) and observed (grey) temperatures (°C) at Sihlsee.

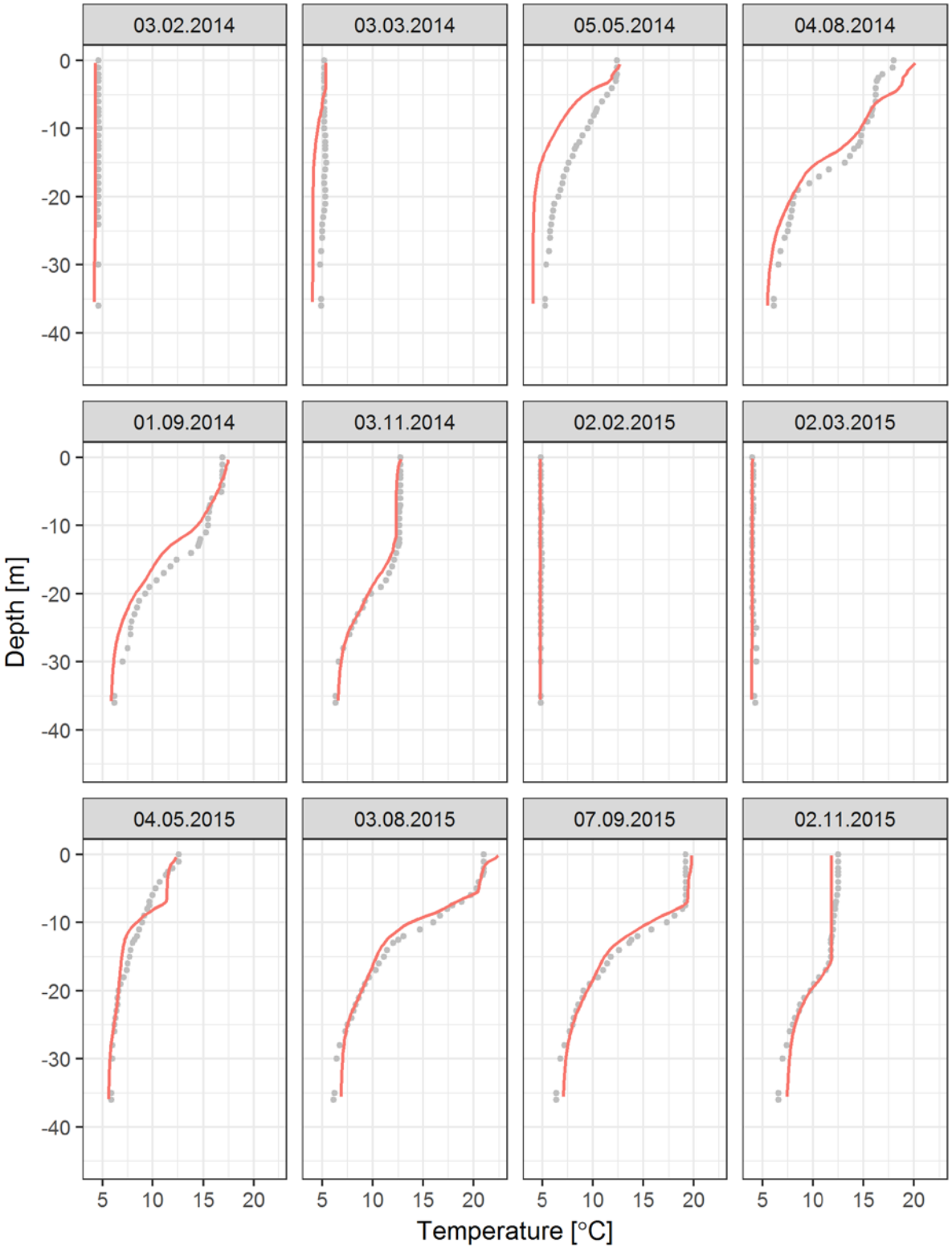

Figure B5. Simulated (red) and observed (grey) temperatures (°C) at Upper Lake Zurich.

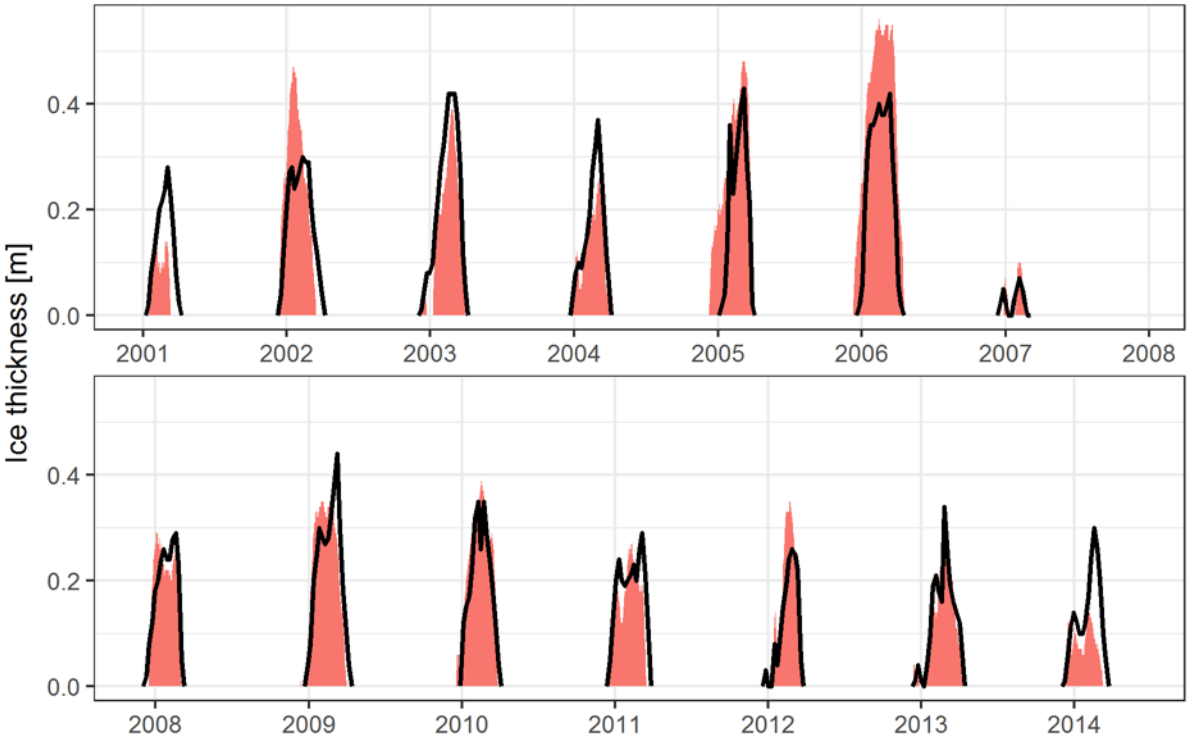

Figure B6. Simulated (red) and observed (black) ice thickness (m) at Sihlsee from 2001-2014.

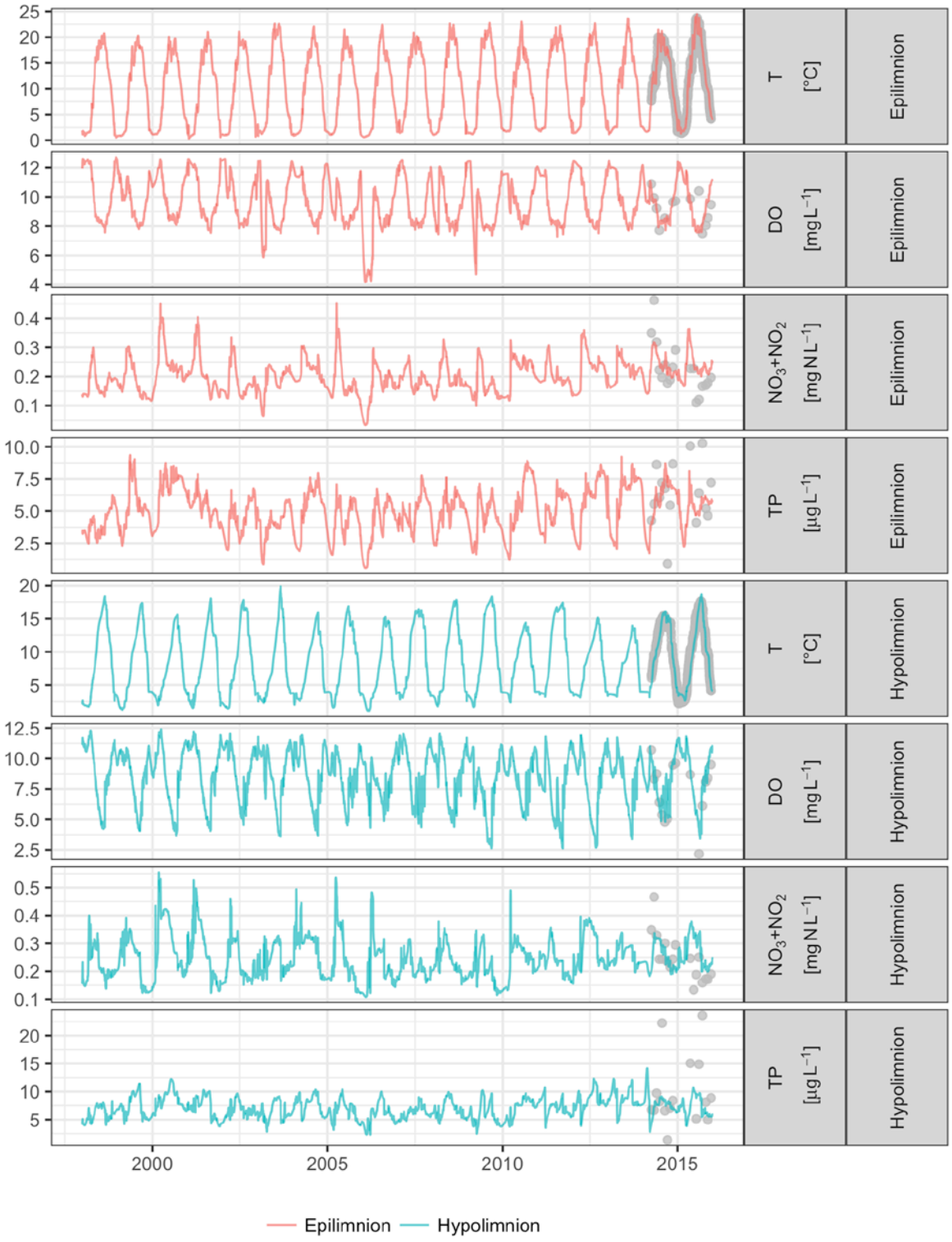

Figure B5. Time series of simulated (lines) and observed (grey points) variables at Sihlsee; depicted are temperature (T) in °C, dissolved oxygen (DO) in mg L^{-1}, sum of nitrate and nitrite (NO_3+NO_2) in µg N L^{-1} and total phosphorus (TP) in µg P L^{-1} all aggregated volumetrically for either epi- (uppermost 5 m of the water column) or hypolimnion (lowermost 5 m of the water column).

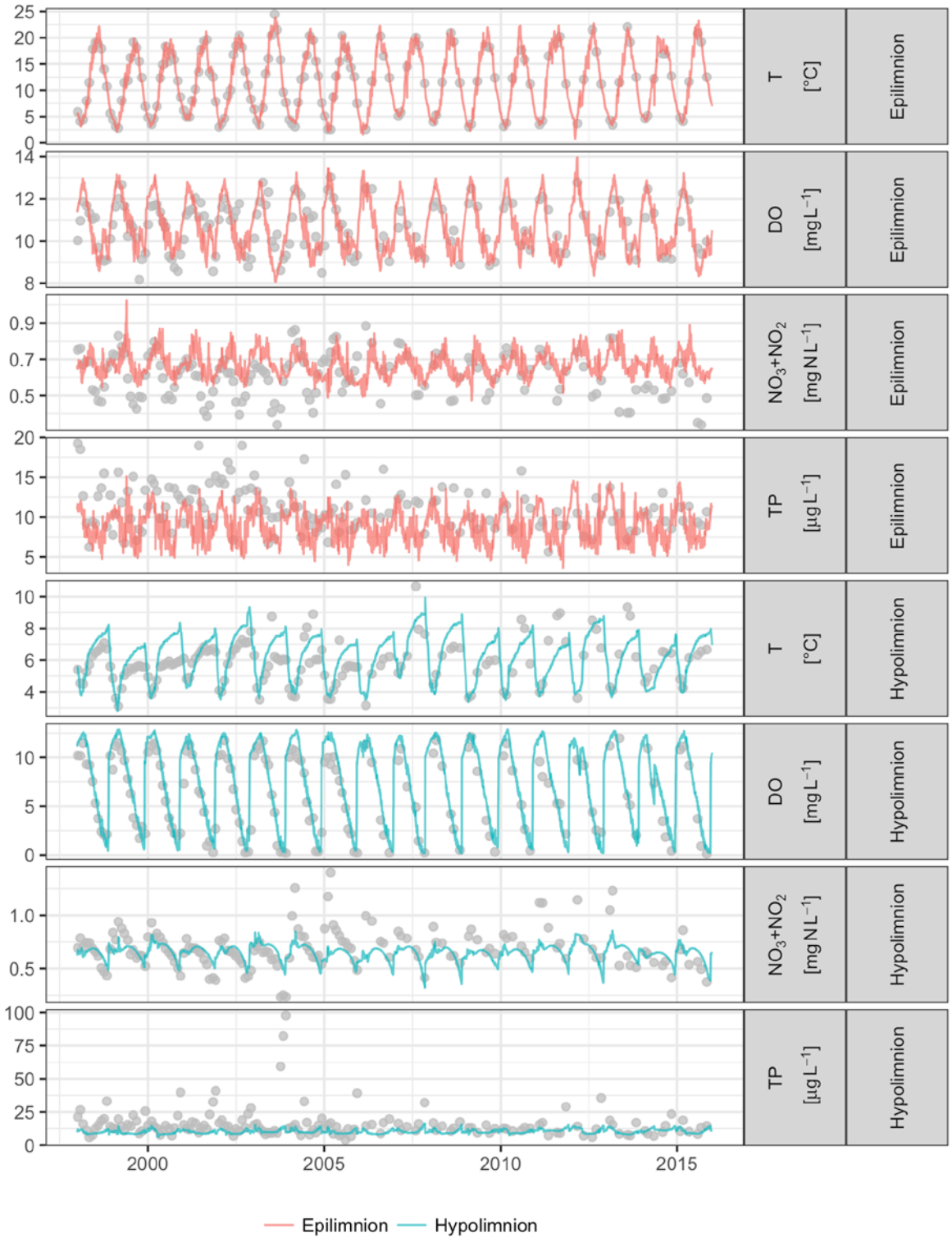

Figure B6. Time series of simulated (lines) and observed (grey points) variables at Upper Lake Zurich; depicted are temperature (T) in °C, dissolved oxygen (DO) in mg L^{-1}, sum of nitrate and nitrite (NO_3+NO_2) in µg N L^{-1} and total phosphorus (TP) in µg P L^{-1} all aggregated volumetrically for either epi- (uppermost 5 m of the water column) or hypolimnion (all depths ≥ 20 m).

C. Results at Upper Lake Zurich

Figure C2 shows the mean and extrema of all considered PS scenarios for Upper Lake Zurich, and Figure C3 shows a boxplot of seasonal differences between either the reference scenario or the extended PS scenario and the present PS scenario. Both figures are separated for epi- and hypolimnion and individually show results for temperature, dissolved oxygen and nutrients.

Effects on temperature in Upper Lake Zurich are minor, with largest deviations in winter (Dec-Feb) due to warmer hypolimnetic water from Sihlsee being released at the surface of Upper Lake Zurich. However, the warming of the entire water column in winter remains at <0.2 °C and <0.5 °C for present PS and extended PS, respectively (Figure C1, Figure C2), since the PS generating flow only accounts to ~10% and ~of natural inflows.

Schmidt stability, which is shown in Figure C3b, is hardly affected due to different PS operations, while the duration of summer stratification lasts ~1 week longer without PS operation, (information is taken from Figure C3a, which shows boxplots of start and end of summer stratification). As a consequence, the dissolved oxygen concentrations in autumn are reduced and the nutrient concentrations are increased without PS operation (Figure C1, Figure C2). The periods with dissolved oxygen concentrations <4 mg L^{-1} span on average ~101, ~100 and ~95 days, for the reference, present PS and extended PS scenarios, respectively. Additionally, the nutrient concentrations of the scenarios with PS are modified by the input of water with different concentrations from the hypolimnion of Sihlsee. Thus, phosphate concentrations are reduced by ~1 and ~2 μg P L^{-1} from November to February for present and extended PS, respectively. The sum of nitrate and nitrite concentrations decrease during the entire year by ~15-50 μg N L^{-1} for both present and extended PS compared to the reference scenario. Between the present and the extended PS scenario the differences remain <15 μg N L^{-1}.

In summary, however, all projected impacts on temperature, stratification, oxygen and nutrient concentrations in Upper Lake Zurich for both the present and the extended PS scenarios do not exceed the interannual variation of these parameters that occur due to variations in meteorology and streamflow. Yet, in the vicinity of the intake/outlet of the PS hydropower plant we cannot exclude the possibility of more relevant effects due to PS operation [16].

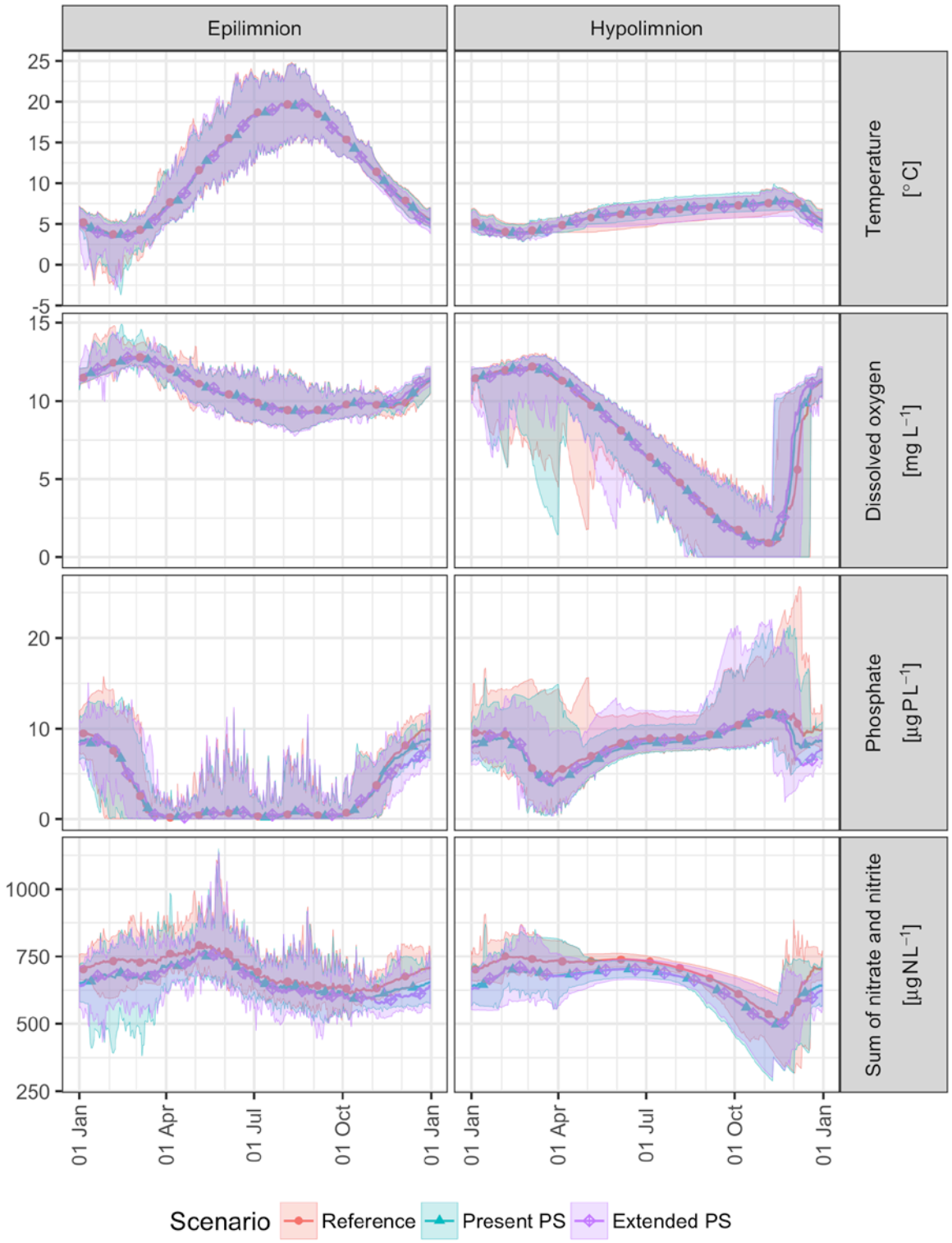

Figure C1. Mean (lines with markers) and range of minima and maxima (shaded areas) of simulated temperature (°C) and concentrations of dissolved oxygen (mg L^{-1}), phosphate (µg P L^{-1}) and the sum of nitrate and nitrite (µg N L^{-1}) for the reference (red), the present PS (green) and the extended PS (blue) scenario at Upper Lake Zurich.

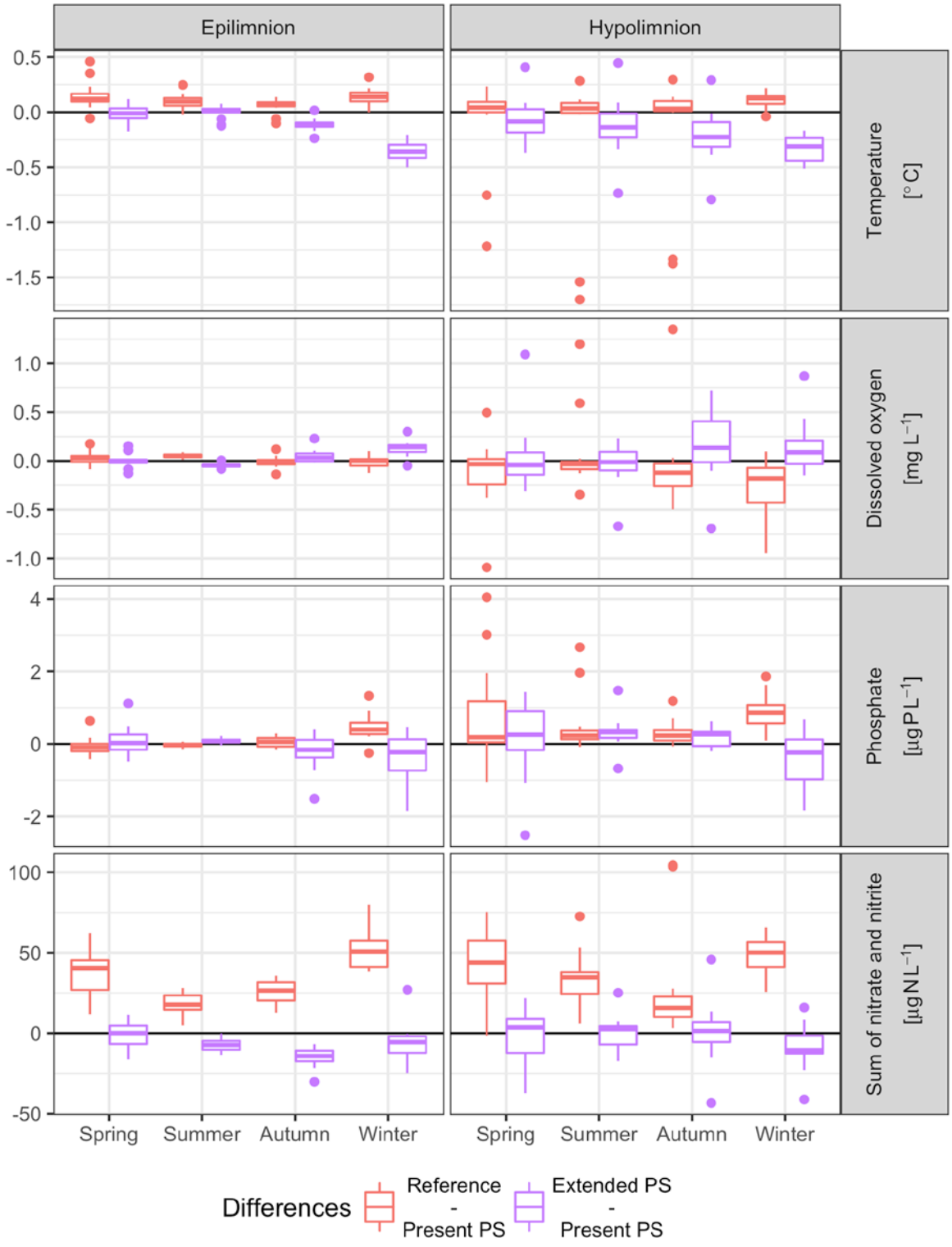

Figure C2. Boxplots of differences in either the reference scenarios or the extended PS scenario to the present PS scenario of temperature (°C) and concentrations of dissolved oxygen (mg L^{-1}), phosphate (µg P L^{-1}) and the sum of nitrate and nitrite (µg N L^{-1}) at Sihlsee. Points show outliers; values were aggregated seasonally for each year before plotting (winter: Dec-Feb, spring: Mar-May, summer: Jun-Aug, autumn: Sep-Nov).

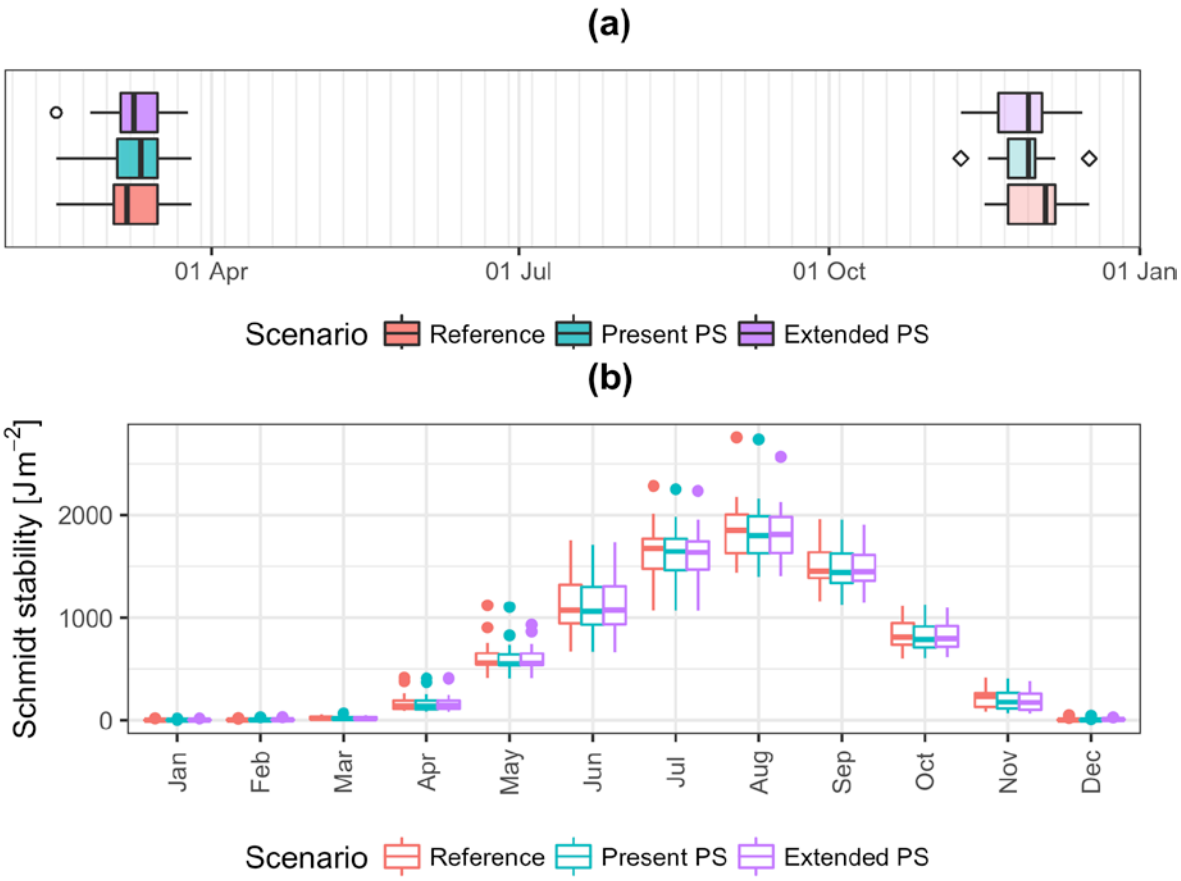

Figure C3. Boxplots for the reference scenario, the present PS and the extended PS scenario at Upper Lake Zurich: (**a**) Start and end of summer stratification; (**b**) Schmidt stability (J m^{-2}), aggregated to monthly mean for each year before plotting. Points show outliers of start (circles) and end (squares) of summer stratification.

D. Specifications of pumped-storage hydropower plants in literature review

Table D1. Specifications of pumped-storage hydropower plants and the connected water bodies (WB) studied in a similar context.

Publication	Head [m]	Volume upper WB [10^6 m^3]	Volume lower WB [10^6 m^3]	Surface area upper WB [km^2]	Surface area lower WB [km^2]	Max. depth upper WB [m]	Max. depth lower WB [m]	Max. PS generation flow [m^3 s^{-1}]	Max. PS pumping flow [m^3 s^{-1}]	Intake/outlet location upper WB	Intake/outlet location lower WB
Bonalumi, *et al.* [14]	~1270	~22	~111	1.43	1.95	26	85	~95	~74	Lower hypolimnion	Upper hypolimnion
Potter, *et al.* [17]	~27	~580 [1]	~407 [1]	~85 [1]	~62 [1]	~33 [1]	~7 [1]	~1347 [2]	~991 [2]	Upper hypolimnion	Upper hypolimnion
USBR [18]	~145	~14	112.6	~1.2 [3]	73	~20 [3]	~27	~112	~97	Lower hypolimnion	Lower hypolimnion
Bermúdez, *et al.* [19]	~283	87 [4]	72 [4]	~7.0	~6.3	~30	~20	~150	~124	Lower hypolimnion	Upper hypolimnion
Anderson [20]	~500	7	74	0.31	13.4	~49	~9	~40	~75		Upper hypolimnion

[1] https://epd.georgia.gov/sites/epd.georgia.gov/files/related_files/site_page/oc5.pdf, 28 February 2018

[2] Estimated with an efficiency of 0.9 and 0.8 for generating and pumping, respectively, from the installed capacities given at http://www.energystorageexchange.org/projects/239, 28 February 2018

[3] https://www.usbr.gov/tsc/techreferences/rec/REC-ERC-82-06.pdf, 28 February 2018

[4] Given is only the storage capacity

References

1. Flerchinger, G.N.; Xaio, W.; Marks, D.; Sauer, T.J.; Yu, Q., Comparison of algorithms for incoming atmospheric long-wave radiation. *Water Resources Research* **2009**, *45*, W03423.

2. Dilley, A.C.; O'Brien, D.M., Estimating downward clear sky long-wave irradiance at the surface from screen temperature and precipitable water. *Quarterly Journal of the Royal Meteorological Society* **1998**, *124*, 1391-1401.

3. Unsworth, M.H.; Monteith, J.L., Long-wave radiation at the ground. *Quarterly Journal of the Royal Meteorological Society* **1975**, *101*, 13-24.

4. Deacon, E.L., The derivation of Swinbank's long-wave radiation formula. *Quarterly Journal of the Royal Meteorological Society* **1970**, *96*, 313-319.

5. Zappa, M.; Andres, N.; Kienzler, P.; Naef-Huber, D.; Marti, C.; Oplatka, M., Crash-Tests for forward-looking flood control in the city of Zürich (Switzerland). *Proc. IAHS* **2015**, *370*, 235-242.

6. Bollrich, G., *Technische Hydromechanik 1*. Verlag Bauwesen: Berlin, **2007**.

7. Keller, H.; Weibel, P., Suspended sediments in streamwater - indicators of erosion and bed load transport in mountainous basins. *IAHS Publication* **1991**, *203*, 53-61.

8. Peters-Kümmerly, B., Untersuchung über Zusammensetzung und Transport von Schwebstoffen in einigen Schweizer Flüssen. *Geographica Helvetia* **1973**, *28*, 137-151.

9. Haynes, W., *CRC Handbook of Chemistry and Physics*. 95 ed.; CRC press.: Boca Raton, FL, **2014**.

10. Gammeter, S.; Forster, R. *Langzeituntersuchungen im Zürichobersee 1972-2000*; Wasserversorgung Zürich: Zürich, **2002**.

11. Der Schweizerische Bundesrat, Gewässerschutzverordnung vom 28. Oktober 1998 (GSchV); SR 814.201; Der Schweizerische Bundesrat: Bern, Switzerland. **1998**.

12. Schildknecht, A.; Köster, O.; Koss, M.; Forster, R.; Leemann, M. *Gewässerzustand von Zürichsee, Zürichobersee und Walensee - Auswertungen der Untersuchungsergebnisse bis 2010, Tech. Bericht der Stadt Zürich*; Wasserversorgung Zürich: Zürich, **2013**.

13. Mieleitner, J.; Reichert, P., Analysis of the transferability of a biogeochemical lake model to lakes of different trophic state. *Ecological Modelling* **2006**, *194*, 49-61.

14. Bonalumi, M.; Anselmetti, F.S.; Wüest, A.; Schmid, M., Modeling of temperature and turbidity in a natural lake and a reservoir connected by pumped-storage operations. *Water Resources Research* **2012**, *48*, WR01184.

15. Mieleitner, J.; Reichert, P., Modelling functional groups of phytoplankton in three lakes of different trophic state *Ecological Modelling* **2008**, *211*, 279-291.

16. Müller, M.; De Cesare, G.; Schleiss, A.J., Flow field in a reservoir subject to pumped-storage operation – in situ measurement and numerical modeling. *Journal of Applied Water Engineering and Research* **2018**, *6*, 109-124.

17. Potter, D.U.; Stevens, M.P.; Meyer, J.L., Changes in physical and chemical variables in a new reservoir due to pumped storage operations. *JAWRA Journal of the American Water Resources Association* **1982**, *18*, 627-633.

18. USBR *Aquatic ecology studies of Twin Lakes, Colorado, 1971-1986: Effects of a pumped-storage hydroelectric project on a pair of montane lakes.*; USBR: Denver, CO, USA, **1993**.

19. Bermúdez, M.; Cea, L.; Puertas, J.; Rodríguez, N.; Baztán, J., Numerical Modeling of the Impact of a Pumped-Storage Hydroelectric Power Plant on the Reservoirs' Thermal Stratification Structure: a Case Study in NW Spain. *Environmental Modeling & Assessment* **2018**, *23*, 71-85.

20. Anderson, M.A., Influence of pumped-storage hydroelectric plant operation on a shallow polymictic lake: Predictions from 3-D hydrodynamic modeling. *Lake and Reservoir Management* **2010**, *26*, 1-13.